

## 1

## The Mössbauer Effect

## 1.1

Resonant Scattering of  $\gamma$ -Rays

It was at the beginning of the 20th century that resonant scattering of light became experimentally verified. For example, when a beam of yellow light (the D-lines) from a sodium lamp goes through a flask with low-pressure sodium vapor in it, sodium atoms in the  $^2\text{S}$  ground state will have a relatively large probability of absorbing the incident photons and making a transition to the excited  $^2\text{P}$  state (as shown in Fig. 1.1). When these atoms return to the ground state, they emit a yellow light of the same wavelength (known as resonance fluorescence) in all spatial directions. In the original direction of the incident beam, the light intensity will be substantially reduced. This phenomenon can be considered as a process of resonant scattering of photons.

In 1929, Kuhn [1] pointed out that a similar  $\gamma$ -ray resonant scattering phenomenon should also exist for the nuclei. However, research during the next twenty plus years failed to produce satisfactory experimental results to support his predictions. The reason was quite clear. Because of the law of momentum conservation, after emitting a  $\gamma$ -ray, the nucleus obtains a velocity in the opposite direction (recoil). Compared to the recoil velocity of an atom when the atom emits a visible photon, the nucleus recoils with a velocity several orders of magnitude larger, takes enough energy away from the emitted  $\gamma$ -ray, and prevents the observation of resonance absorption. We will now discuss this in detail.

Suppose a free nucleus of mass  $M$  and initial velocity  $v$  is in the excited state  $E_e$ , emitting a  $\gamma$ -ray in the  $x$ -direction when it returns to the ground state. Figure 1.2 shows the energy levels and recoil of the nucleus, where  $v_x$  is the  $x$ -component of the initial velocity and  $v_R$  its recoil velocity (relative to  $v_x$ ). According to momentum conservation and energy conservation, we have

$$\begin{cases} Mv_x = \frac{E_\gamma}{c} + M(v_x - v_R) \\ E_e + \frac{1}{2}Mv_x^2 = E_g + E_\gamma + \frac{1}{2}M(v_x - v_R)^2 \end{cases} \quad (1.1)$$

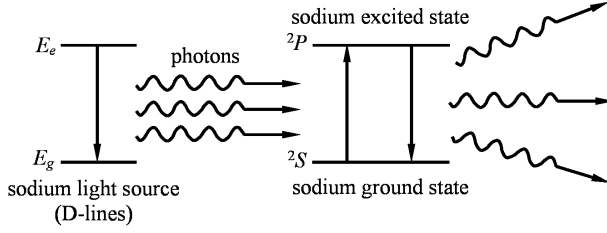


**Fig. 1.1** Schematic diagram of resonance scattering of light.

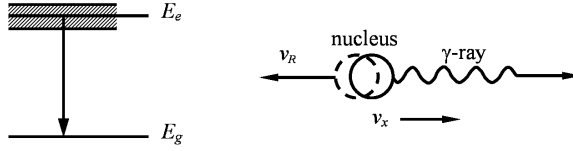


**Fig. 1.2** Recoil of a nucleus after emitting a  $\gamma$ -ray.

where  $E_g$  is the ground state energy of the nucleus and  $E_\gamma$  is the energy of the emitted  $\gamma$ -ray. From the above equations, we obtain

$$E_\gamma = (E_e - E_g) - \frac{1}{2} M v_R^2 + M v_x v_R = E_0 - E_R + E_D, \quad (1.2)$$

where  $E_0$  is the energy difference between the excited state and the ground state

$$E_0 = E_e - E_g, \quad (1.3)$$

$E_R$  is the recoil energy

$$E_R = \frac{1}{2} M v_R^2 = \frac{E_\gamma^2}{2 M c^2}, \quad (1.4)$$

and  $E_D$  depends on the initial velocity  $v_x$  and is due to the Doppler effect (known as the Doppler energy shift)

$$E_D = M v_x v_R = \frac{v_x}{c} E_\gamma. \quad (1.5)$$

We will now consider the following two cases ( $v_x = 0$  and  $v_x \neq 0$ ) separately.

(a) If  $v_x = 0$ , then  $E_D = 0$ . In this case, the excited nucleus is at rest. The energy spectrum of the emitted  $\gamma$ -rays from such nuclei is shown by the dashed line in Fig. 1.3. The spectrum is a sharp peak centered at  $E_0 - E_R$ , and its width at

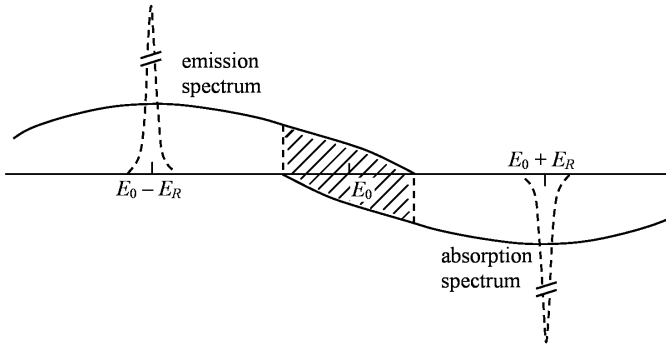


**Fig. 1.3** Emission and absorption  $\gamma$ -ray spectra when recoil is present.

the half height is nearly the same as the natural width ( $\Gamma_n$ ) of the excited energy level.

The nuclei in the ground state ( $E_g$ ) may resonantly absorb the incident  $\gamma$ -rays and transit to the excited state ( $E_e$ ). The energy distribution of these absorbed  $\gamma$ -rays is identical to the emission spectrum, except for a shift of  $E_R$  to the right of  $E_0$ , as shown in Fig. 1.3. The energy difference between the emitted and the absorbed  $\gamma$ -rays is  $2E_R$ . Therefore, the fundamental condition necessary for the photon's resonant scattering is

$$\frac{\Gamma_n}{2E_R} > 1, \quad (1.6)$$

that is, the recoil energy must be less than half of the natural width of the excited state. Comparing the data for the  $^{57}\text{Fe}$  nucleus and the sodium atom in Table 1.1, we can easily see that for the Na atom, condition (1.6) is completely satisfied, because the emission spectrum and the absorption spectrum are almost overlapping, resulting in very large probability for resonant absorption. For the  $^{57}\text{Fe}$  nucleus, however, its  $\Gamma_n/2E_R$  value is far from satisfying condition (1.6). Although the natural widths  $\Gamma_n$  of a nucleus and an atom are comparable, the former gives a much more energetic photon than the latter, usually by three orders of magni-

**Table 1.1** Comparison between photon emissions from the  $^{57}\text{Fe}$  nucleus and the Na atom while each decays from its first excited state to the ground state.

	$E_\gamma(\text{eV})$	$\Gamma_n(\text{eV})$	$E_R(\text{eV})$	$\Gamma_n/2E_R$
$^{57}\text{Fe}$ nucleus	$14.4 \times 10^3$	$4.65 \times 10^{-9}$	$1.95 \times 10^{-3}$	$1.2 \times 10^{-6}$
Na atom (D-lines)	2.1	$4.39 \times 10^{-8}$	$1.0 \times 10^{-10}$	$2.2 \times 10^2$

tude. This makes their  $E_R$  values differ by more than six orders of magnitude, and this is the reason why resonant absorption of  $\gamma$ -rays is usually not observed.

(b) For  $v_x \neq 0$ , the situation is more common. Because of the random thermal motions of free atoms, their velocities  $v_x$  may have large variations, described by the Maxwell distribution

$$p(v_x) dv_x = \left( \frac{M}{2\pi k_B T} \right)^{1/2} \exp\left( -\frac{M}{2k_B T} v_x^2 \right) dv_x$$

where  $k_B$  is Boltzmann's constant and  $T$  is the absolute temperature. This distribution will greatly broaden the emission spectrum (or the absorption spectrum), as indicated by the solid line in Fig. 1.3. This broadening is due to the Doppler effect, and hence is known as Doppler broadening. Since the width of the above velocity distribution is  $2(2k_B T \ln 2/M)^{1/2}$ , the width of the emission spectral line is then

$$\Delta E_D = M v_R \left( 2\sqrt{\frac{2k_B T \ln 2}{M}} \right) = 4\sqrt{E_R k_B T \ln 2}. \quad (1.7)$$

For  $^{57}\text{Fe}$  at  $T = 300 \text{ K}$ ,  $\Delta E_D = 2.4 \times 10^{-2} \text{ eV} > 2E_R$ . This means that the emission spectrum partially overlaps the absorption spectrum (the shaded region in Fig. 1.3), and it may be possible to observe some effect of resonant absorption.

## 1.2

### The Mössbauer Effect

#### 1.2.1

##### Compensation for Recoil Energy

As discussed above, if the nucleus is free to move, the lost energy due to recoil must be compensated before substantial resonance absorption of  $\gamma$ -rays can be observed. Several ingenious experiments were devised to achieve this compensation, two of which are briefly explained here.

The first experiment made use of mechanical motion of the source [2]. The radioactive source was mounted on the tip of a high-speed rotor. Due to the Doppler effect, the  $\gamma$ -rays acquired an additional energy  $\Delta E$ ,

$$\Delta E = \frac{v}{c} E_\gamma. \quad (1.8)$$

It was possible to adjust the speed  $v$  of the rotor to completely compensate the recoil energy loss, i.e.,  $(v/c)E_\gamma = 2E_R$  (for  $^{57}\text{Fe}$ ,  $v = 81 \text{ m s}^{-1}$ ). This experiment had two problems. First, only during a very short portion of the rotation period could the emitted  $\gamma$ -rays be used in the experiment, and thus the source was largely under-utilized. Second, the experiment was limited by the maximum ob-

tainable speed of the mechanical rotor and especially by the poor stability of the rotor speed.

The second experiment used the fact described in Eq. (1.7) that the Doppler broadening is increased by raising the temperature. As a result, it would cause increases in the overlapping region in Fig. 1.3, and therefore increases in the probability of resonance absorption.

By the above means, the phenomenon of  $\gamma$ -ray resonant absorption had been observed before 1954, but a major shortcoming was that these resonance absorption experiments all involved recoil, which would never be practically significant due to low  $\gamma$ -ray counts and poor energy resolution. A historic discovery by Mössbauer of resonant absorption *without* recoil completely eliminated the need for the above effort to compensate the energy loss. We will now describe this discovery.

### 1.2.2

#### The Discovery of the Mössbauer Effect

In 1958, Rudolf L. Mössbauer [3] was investigating the resonant absorption of the 129 keV  $\gamma$ -ray in  $^{191}\text{Ir}$  nucleus and discovered that if the source nuclei  $^{191}\text{Os}$  and absorber nuclei  $^{191}\text{Ir}$  were rigidly bound in crystal lattices, the recoil could be effectively eliminated and the resonant absorption was readily observed.

In a crystal lattice, an atom is held in its equilibrium position by strong chemical bonds corresponding to an energy of typically 10 eV. For the 129 keV transition in free  $^{191}\text{Ir}$  nucleus (Fig. 1.4), the recoil energy is  $4.7 \times 10^{-2}$  eV, much smaller than the chemical bond energy. Therefore, from the classical viewpoint, when the  $\gamma$ -ray is emitted by a nucleus bound in a lattice, the nucleus will not recoil alone, but the entire crystal lattice recoils together (a total of about  $10^{18}$  atoms). In this case, the mass  $M$  in the denominator of Eq. (1.4) should be the mass of the whole crystal, not the individual nucleus. This reduces the recoil energy to a negligible amount ( $\sim 10^{-20}$  eV). Consequently, Eq. (1.6) is satisfied, Eq. (1.2) is simplified to  $E_\gamma \approx E_0$ , and the entire process becomes a recoilless resonant absorption. A more exact explanation of this phenomenon is given by a quantum mechanical description in Section 1.5.

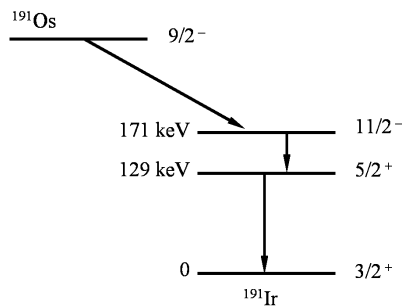


Fig. 1.4 Decay scheme of  $^{191}\text{Os}$ .

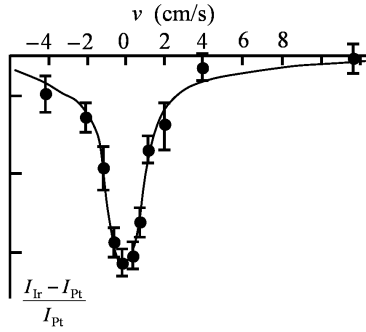
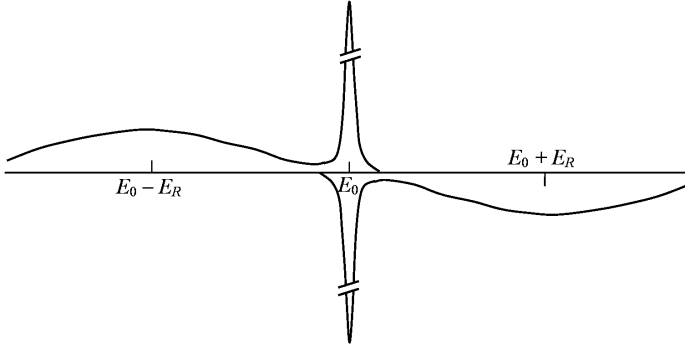


Fig. 1.5 Resonance absorption curve of the 129 keV  $\gamma$ -rays by  $^{191}\text{Ir}$ .

In Mössbauer's first experiment where he observed recoilless resonance absorption of  $\gamma$ -rays, the radiation source was a crystal containing  $^{191}\text{Os}$  and the absorber was an iridium crystal, both at a temperature of 88 K. A platinum (Pt) comparison absorber of the same thickness was used to measure the background. Because the process was recoilless, the Doppler velocity only needed to be small, about several centimeters per second. The results from that first experiment are reproduced in Fig. 1.5, where the horizontal axis represents the  $\gamma$ -ray energy variation  $\Delta E$  (or source velocity  $v$ ). When the source is moving towards the absorber,  $v > 0$ , and when the source is moving away from the absorber,  $v < 0$ . The vertical axis represents the relative change in the  $\gamma$ -ray intensity,  $(I_{\text{Ir}} - I_{\text{Pt}})/I_{\text{Pt}}$ , where  $I_{\text{Ir}}$  and  $I_{\text{Pt}}$  are the  $\gamma$ -ray intensities transmitted through the Ir and Pt absorbers, respectively.

As shown in Fig. 1.5 and pointed out by Mössbauer, the width of the spectrum is  $4.6 \times 10^{-6}$  eV, which is just slightly more than twice the natural width of the 129 keV energy level of  $^{191}\text{Ir}$ . Never before had such a high resolution in energy ( $\Delta E/E \approx 3.5 \times 10^{-11}$ ) been achieved, and Mössbauer's research results were fundamentally different from what anyone had previously obtained from  $\gamma$ -ray resonant scattering, because he observed  $\gamma$ -ray emission and absorption events in which the recoil was completely absent. Not too long after the discovery of recoilless  $\gamma$ -ray emission and resonant absorption, this effect was named after its discoverer and is now known as the Mössbauer effect.

In reality, the Mössbauer nucleus is not rigidly bound, but is usually free to vibrate about its equilibrium position. Photons may exchange energy with the lattice, resulting in the creation or annihilation of quanta (phonons) of lattice vibrations. Suppose we have an Einstein solid with one vibrational frequency  $\omega$ , then the lattice can only receive or release energies in integral multiples of  $\hbar\omega$  ( $0, \pm\hbar\omega, \pm 2\hbar\omega, \dots$ ). So if  $E_{\text{R}} < \hbar\omega$ , the lattice cannot absorb the recoil energy, i.e., the zero phonon process, and the  $\gamma$ -ray is emitted without recoil. The probability of having such a process is known as the recoilless fraction  $f$ , an extremely important parameter in Mössbauer spectroscopy.



**Fig. 1.6** Emission and absorption spectra of  $\gamma$ -rays when  $E_R \ll \hbar\omega$ .

In a typical lattice, both  $E_R$  and  $\hbar\omega$  are in the ranges  $10^{-3}$  to  $10^{-1}$  eV. Obviously, the value of  $f$  depends on how  $E_R$  compares with  $\hbar\omega$ . Only when  $E_R \ll \hbar\omega$  will  $f$  be reasonably large (see Fig. 1.6). As we derive it later (see Section 1.5.4), according to Lipkin's sum rule, when a large number of absorption events are considered, the average energy transferred to the lattice must be exactly equal to  $E_R$ . Let a total of  $m$   $\gamma$ -photons with  $E_\gamma$  be absorbed among which  $n$  of them cause zero phonon creation and the rest  $(m - n)$  photons each excites a single phonon (neglecting double phonons), then

$$mE_R = (m - n)\hbar\omega.$$

Based on the Einstein model, we arrive at an approximate expression for the recoilless fraction

$$f = \frac{n}{m} = 1 - \frac{E_R}{\hbar\omega}. \quad (1.9)$$

It can be seen from this expression that, in order to observe the Mössbauer effect, the recoilless fraction  $f$  should be sufficiently large, and we would like to have the following condition between  $E_R$  and  $\hbar\omega$ :

$$E_R \ll \hbar\omega. \quad (1.10)$$

A more precise expression for the recoilless fraction is

$$f = e^{-k^2 \langle x^2 \rangle}$$

where  $\langle x^2 \rangle$  is the mean square displacement of a nucleus along the direction of the wave vector  $\mathbf{k}$  of the emitted  $\gamma$ -ray. This expression points out that in a liquid

or a gas, the Mössbauer effect is extremely difficult to observe because of the large  $\langle x^2 \rangle$  values. Also, a small  $k$  value would give a large  $f$  value, and therefore  $\gamma$ -rays with lower energies will favor the observation of the Mössbauer effect. At present, the Mössbauer effect has been observed from more than 100 nuclear isotopes (e.g.,  $^{57}\text{Fe}$ ,  $^{119}\text{Sn}$ ,  $^{191}\text{Ir}$ , etc.), among which one of the highest  $\gamma$ -ray energies is 187 keV in  $^{190}\text{Os}$ . For a  $\gamma$ -ray energy higher than 100 keV, the source and the absorber are usually kept at low temperatures to reduce their  $\langle x^2 \rangle$  values.

### 1.3

#### The Mössbauer Spectrum

##### 1.3.1

##### The Measurement of a Mössbauer Spectrum

To facilitate our discussions in the first two chapters, the basic principles of measuring a Mössbauer spectrum will be given, before the experimental details in Chapter 3.

The shape of a resonance curve is often used to characterize the properties of the resonance system. For example, we can obtain the natural width  $\Gamma_n$  of the excited energy state from the linewidth of the measured  $\gamma$ -ray resonance curve and estimate the life time of the energy state according to the uncertainty relation  $\tau\Gamma_n \sim \hbar$ . A Mössbauer spectrum is a recoil-free resonance curve. To measure this, we no longer need those high-speed rotors, but it is still necessary to use the Doppler effect for modulating the  $\gamma$ -ray energy  $E_\gamma$  within a small energy range,  $E_\gamma(1 \pm v/c)$ . A velocity transducer with the mounted source moves with respect to the absorber and the emitted  $\gamma$ -ray energy is therefore modulated, as shown in Fig. 1.7. A Mössbauer absorption spectrum, shown on the right of Fig. 1.7, is a record of transmitted  $\gamma$ -ray counts through the absorber as a function of  $\gamma$ -ray energy, whose linewidth has a minimum value of  $\Gamma_s + \Gamma_a$  (the sum of the natural widths of the Mössbauer nuclei in the source and the absorber).

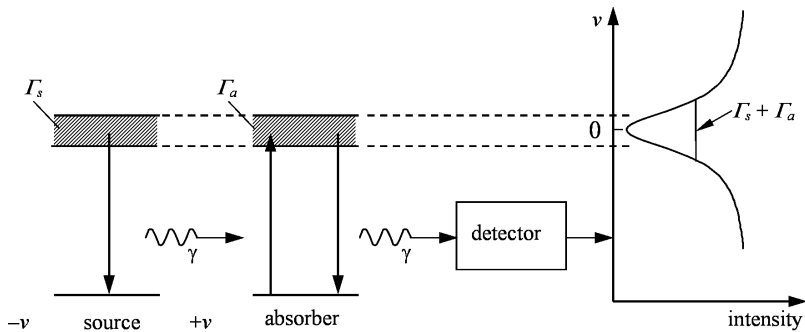


Fig. 1.7 Measuring a Mössbauer spectrum.

For the sake of simplicity, it is customary to use the source velocity (in  $\text{mm s}^{-1}$ ) to label the energy axis. To obtain the energy value, one simply multiplies the velocity by a constant  $E_\gamma/c$ , and for  $^{57}\text{Fe}$ ,  $E_\gamma/c = 4.8075 \times 10^{-8} \text{ eV mm}^{-1} \text{ s}$ .

### 1.3.2

#### The Shape and Intensity of a Spectral Line

After a Mössbauer resonant absorption, the nuclear excited state is an isomeric state, which can only decay to the ground state through  $\gamma$ -ray emission or internal conversion. The cross-section of resonant absorption of  $\gamma$ -rays (as a function of photon energy  $E$ ) is described by the Breit–Wigner formula [1, 4]:

$$\sigma_a(E) = \frac{\sigma_0 \Gamma_a^2/4}{(E - E_0)^2 + \Gamma_a^2/4} \quad (1.11)$$

where

$$\sigma_0 = \frac{\lambda^2}{2\pi} \frac{1 + 2I_e}{1 + 2I_g} \frac{1}{1 + \alpha} \quad (1.12)$$

is the maximum resonance cross-section,  $E_0$  and  $\lambda$  are the energy and wavelength of the  $\gamma$ -ray,  $I_e$  and  $I_g$  are, respectively, the nuclear spins of the excited and the ground states, and  $\alpha$  is the internal conversion coefficient.

Because its excited state has a certain width  $\Gamma_s$ , the emitted  $\gamma$ -rays from the source are not completely monochromatic, but follow the Lorentzian distribution around  $E_0$

$$\mathcal{L}(E) dE = \frac{\Gamma_s}{2\pi} \frac{1}{(E - E_0)^2 + \Gamma_s^2/4} dE \quad (1.13)$$

where

$$\int \mathcal{L}(E) dE = 1. \quad (1.14)$$

Therefore, in a situation where both the source and the absorber are very thin, the observed resonance absorption curve can be calculated by a convolution integral

$$\sigma_a^{\text{exp}}(E) \propto \int_{-\infty}^{+\infty} \mathcal{L}(E - x) \sigma(x) dx = \frac{\sigma_0 \Gamma_a}{\Gamma_a + \Gamma_s} \frac{\left(\frac{\Gamma_s + \Gamma_a}{2}\right)^2}{(E - E_0)^2 + \left(\frac{\Gamma_s + \Gamma_a}{2}\right)^2} \quad (1.15)$$

and it is clear that the line shape is also Lorentzian, similar to Eq. (1.13) except that the linewidth becomes  $\Gamma_s + \Gamma_a$ . In reality, because of the finite thicknesses of the source and absorber, the emission and absorption spectral linewidths  $\Gamma_s$

and  $\Gamma_a$  would be larger than the natural width  $\Gamma_n$  (for  $^{57}\text{Fe}$ ,  $\Gamma_n \approx 0.097 \text{ mm s}^{-1}$ ), and the observed resonance line would be broader than  $2\Gamma_n$ .

We now discuss in detail how the thickness of an absorber influences the shape and intensity of a transmission spectrum. Let the total intensity of the  $\gamma$ -ray emitted by Mössbauer nuclei be  $I_0$ , of which only a part  $I_r$  is recoil free and distributed according to a Lorentzian shape:

$$I_r(E, v, 0) = f_s I_0 \mathcal{L}\left(E - \frac{v}{c} E_0\right)$$

where  $f_s$  and  $v$  are the recoilless fraction and the Doppler velocity of the source. Going through the absorber,  $\gamma$ -ray intensity is reduced because of two absorption processes, a non-resonance atomic absorption (mainly the photoelectric effect) with a mass absorption coefficient of  $\mu_a$  ( $\mu_a$  values for different elements are tabulated in Appendix H) and a Mössbauer resonance absorption with an absorption coefficient of  $\mu_r$ :

$$\mu_r(E) = n_a f \sigma_a(E) \quad (1.16)$$

where  $n_a$  is the number of Mössbauer nuclei in the absorber per unit mass and  $f$  is the recoilless fraction of the absorber. Considering both of these absorption processes, the  $\gamma$ -ray intensity decreases exponentially after transmitting an absorber thickness  $d$  ( $\text{mg cm}^{-2}$ ):

$$I_r(E, v, d) = f_s I_0 \mathcal{L}\left(E - \frac{v}{c} E_0\right) e^{-(\mu_a + \mu_r)d}. \quad (1.17)$$

According to this, at a given Doppler velocity of the source, the intensity of the recoil-free  $\gamma$ -ray detected should be an integral over the energy:

$$I_r(v, d) = \int_{-\infty}^{+\infty} I_r(E, v, d) dE = f_s I_0 e^{-\mu_a d} T(v) \quad (1.18)$$

where

$$T(v) = \int_{-\infty}^{+\infty} \mathcal{L}\left(E - \frac{v}{c} E_0\right) A(E) dE, \quad (1.19)$$

$$A(E) = \exp[-\mu_r(E)d] = \exp[-\sigma(E)t_a], \quad (1.20)$$

$$\sigma(E) = \sigma_a(E)/\sigma_0,$$

$$t_a = n_a f \sigma_0 d. \quad (1.21)$$

$T(v)$  is known as the transmission integral. As defined in Eq. (1.21),  $t_a$  is called the effective thickness of the absorber, and is temperature dependent in the same manner as  $f$ .

The rest of the  $\gamma$ -rays are emitted with recoil, and they are distributed in a rather broad energy range (Fig. 1.6) and absorbed solely due to the non-resonant absorption process. Thus, the intensity after absorption is independent of the Doppler velocity  $v$  and can be expressed as

$$I(d) = I_0(1 - f_s)e^{-\mu_a d}. \quad (1.22)$$

Combining Eqs. (1.18) and (1.22), we obtain the total intensity recorded by the detector (whose efficiency is assumed to be 100%) as

$$I(v, d) = I_r(v, d) + I(d) = I(\infty, d)[1 - f_s + f_s T(v)] \quad (1.23)$$

where  $I(\infty, d) = I_0 \exp(-\mu_a d)$  is the spectral baseline corresponding to  $v = \infty$ .

If we neglect hyperfine interactions for the time being, the fractional intensity of the absorbed of  $\gamma$ -rays at a Doppler velocity  $v$  can be defined as

$$\varepsilon(v) = \frac{I(\infty, d) - I(v, d)}{I(\infty, d)} = f_s[1 - T(v)] \quad (1.24)$$

which describes the shape of the absorption spectrum. According to Appendix A or Ref. [5], the fractional intensity  $\varepsilon(v)$  can be obtained analytically and, at resonance  $v = v_r = 0$ ,  $\varepsilon(v)$  reaches its maximum

$$\frac{\varepsilon(v_r)}{f_s} = 1 - e^{-t_a/2} I_0\left(\frac{t_a}{2}\right) - 2e^{-t_a/2} \sum_{n=1}^{\infty} \left(\frac{\xi - 1}{\xi + 1}\right)^n I_n\left(\frac{t_a}{2}\right) \quad (1.25)$$

which is explicitly expressed in terms of  $\xi = \Gamma_s/\Gamma_a$ . In the above equation,  $I_n$  is the modified Bessel function of the first kind of order  $n$ . If  $\Gamma_s = \Gamma_a$ , thus  $\xi = 1$ , Eq. (1.25) becomes

$$\varepsilon(v_r) = f_s \left[ 1 - e^{-t_a/2} I_0\left(\frac{t_a}{2}\right) \right] \quad (1.26)$$

which is a well-known result independent of both linewidths.

Next, we discuss the contribution of the third term in  $\varepsilon(v_r)$ , which will be abbreviated as  $\varepsilon_3$ :

$$\varepsilon_3 = -2e^{-t_a/2} \sum_{n=1}^{\infty} \left(\frac{\xi - 1}{\xi + 1}\right)^n I_n\left(\frac{t_a}{2}\right). \quad (1.27)$$

The value of  $\varepsilon(v_r)/f_s$  in Eq. (1.25) is plotted in Fig. 1.8 as a function of  $t_a$  and  $\xi$ . Regardless whether  $n$  is even or odd,  $I_n(t_a/2)$  is always positive. Therefore, the sign of  $\varepsilon_3$  is determined by the factor  $(\xi - 1)/(\xi + 1)$ . When  $\xi < 1$ ,  $\varepsilon_3 > 0$ , and when  $\xi > 1$ ,  $\varepsilon_3 < 0$ . The effect of this third term  $\varepsilon_3$  is clearly demonstrated in

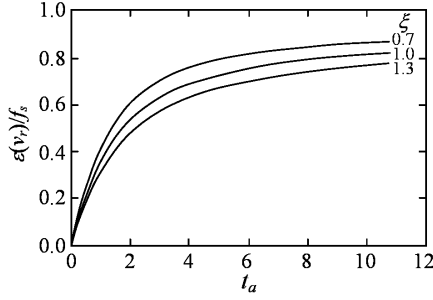


Fig. 1.8  $\varepsilon(v_r)/f_s$  as a function of  $t_a$  for  $\zeta = 0.7, 1.0$ , and  $1.3$  [5].

Fig. 1.8. The curve with  $\zeta = 1$  is completely consistent with those given in Ref. [6]. In practice, cases with  $\zeta > 1$  are hardly observed and  $\zeta < 1$  is in the majority. Therefore, the influence of the third term on  $\varepsilon(v_r)$  is essentially the addition of a positive contribution. Obviously, when  $t_a < 1$ , such an influence becomes negligible regardless of the value of  $\zeta$ .

In fact, the above argument can be understood in the following straightforward way. In the case where  $\Gamma_s < \Gamma_a$  (or  $\zeta < 1$ ), the absorber in some sense looks like a “black absorber” [7] absorbing the majority of resonant  $\gamma$ -rays. In other words, the resonant  $\gamma$ -rays, as a whole, have a higher probability of becoming absorbed.

Based on the above results, a transmission Mössbauer spectrum is sketched in Fig. 1.9 where  $I_b$  represents the background counts. During the above derivation, we assumed that the intensity was corrected by  $I_b$ .

As long as the “thin absorber approximation” ( $t_a < 1$ ) is valid, one only need to take the first two terms in the polynomial expansion of  $A(E)$  in Eq. (1.20). Then the fractional absorption intensity described in Eq. (1.24) can be easily written as

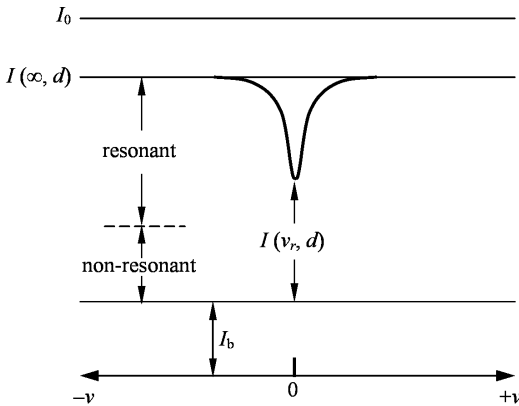


Fig. 1.9 Contributions to the Mössbauer spectrum in transmission geometry.

$$\begin{aligned}
\varepsilon(v) &= f_s [1 - T(v)] = f_s \int_{-\infty}^{+\infty} \mathcal{L}\left(E - \frac{v}{c} E_0\right) \left[1 - \exp\left(-\frac{t_a \sigma_a}{\sigma_0}\right)\right] dE \\
&\approx f_s \int_{-\infty}^{+\infty} \mathcal{L}\left(E - \frac{v}{c} E_0\right) \frac{t_a (\Gamma_a/2)^2}{(E - E_0)^2 + (\Gamma_a/2)^2} dE \\
&= \frac{\Gamma_a}{\Gamma_s + \Gamma_a} \frac{f_s t_a \left(\frac{\Gamma_s + \Gamma_a}{2}\right)^2}{\left(\frac{v}{c} E_0\right)^2 + \left(\frac{\Gamma_s + \Gamma_a}{2}\right)^2}.
\end{aligned} \tag{1.28}$$

This means when  $t_a < 1$ , the spectral shape is still Lorentzian. At resonance, expression (1.25) becomes identical to (1.28), only if  $t_a < 1$  and  $\Gamma_s = \Gamma_a$ . The area of the absorption spectrum has been accurately calculated [4]:

$$A(t_a) = f_s \Gamma_a \pi \frac{t_a}{2} \exp\left(-\frac{t_a}{2}\right) \left[ J_0\left(i \frac{t_a}{2}\right) + J_1\left(i \frac{t_a}{2}\right) \right] \tag{1.29}$$

where  $J_0$  and  $J_1$  are the zeroth- and first-order Bessel functions. Important parameters of a Mössbauer spectrum are the height, width, area, and position of a spectral line. Because of the constraint in Eq. (1.29), only two of the first three parameters are independent.

As the absorber thickness increases, the area  $A(t_a)$ , as well as  $\varepsilon(v_r)$ , deviates considerably from its linearity with  $t_a$  and gets saturated (see Figs. 1.10 and 1.8). Interpretation of Mössbauer spectra is often complicated by such a saturation effect due to a finite absorber thickness. A comparison between Figs. 1.10 and 1.8 shows how the area  $A(t_a)$  saturates much less rapidly than  $\varepsilon(v_r)$ . A further analysis reveals that the spectral shape remains Lorentzian for up to  $t_a \approx 10$ .

Notice that  $\varepsilon(v)$  describes the shape of the spectrum and obviously depends on both  $\Gamma_s$  and  $\Gamma_a$ , while the area  $A(t_a)$  is an integral of  $\varepsilon(v)$  over the Doppler velocity range (see Appendix A) and is only dependent on  $\Gamma_a$ .

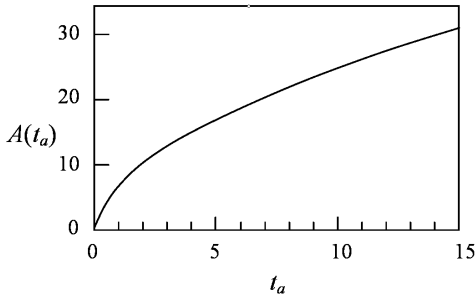


**Fig. 1.10**  $A(t_a)$  as a function of  $t_a$ . In plotting this curve, the proportionality constant ( $f_s \Gamma_a \pi$ ) in Eq. (1.29) is taken to be 1.

## 1.4

**The Classical Theory**

Although the Mössbauer effect is a quantum mechanical effect, its main features can be also derived by the classical theory. The first comprehensive classical description was provided by Shapiro [8]. A radioactive nucleus, as a classical oscillator, does not experience a recoil effect and emits an electromagnetic wave of frequency  $\omega_0$ . The distribution in frequency is entirely determined by the Doppler effect. Thus, the corresponding vector potential at distance  $x_0$  from the source is then

$$\mathbf{A}(t) = \mathbf{A}(0) \exp(-\gamma t) \exp[i(\omega_0 t - kx_0)] \quad (1.30)$$

where  $\gamma$  is the damping coefficient, which is half of the natural width of the excited state,  $\gamma = \Gamma_n/2$ . If thermal motion of the nucleus is neglected, the distance  $x_0$  will be constant. As a result, leaving out the last phase factor in Eq. (1.30) has no effect on the recoilless fraction. Thus the radiation intensity as a function of frequency is

$$I(\omega) = I_0 \frac{(\Gamma_n/2)^2}{(\omega_0 - \omega)^2 + (\Gamma_n/2)^2}. \quad (1.31)$$

In reality, the nucleus in a solid undergoes inevitable thermal motion around its equilibrium position. From the classical point of view, this motion modulates the electromagnetic wave due to the Doppler effect. Let  $v(t)$  be the velocity component of the nucleus in the direction of  $\gamma$ -ray propagation. The phase of the wave is modulated and becomes

$$\phi(t) = \int_{-\infty}^t \omega_0 \left( 1 + \frac{v(t')}{c} \right) dt' = \omega_0 t + \frac{2\pi x(t)}{\lambda} \quad (1.32)$$

where  $x(t)$  is the instantaneous displacement of the nucleus away from its equilibrium position in the direction of the  $\gamma$ -ray propagation, and may be expressed as

$$x(t) = x_0 \sin \Omega t \quad (1.33)$$

where we have used  $\Omega$  ( $\Omega \ll \omega_0$ ) to represent the frequency of the thermal motion of all Mössbauer nuclei (as is the case with the Einstein model). Incorporating the phase modulation into Eq. (1.30), the vector potential becomes

$$\mathbf{A}(t) = \mathbf{A}(0) \exp(-i\omega_0 t - \Gamma_n t/2) \exp(ikx_0 \sin \Omega t). \quad (1.34)$$

If we expand the last phase factor into a sum of Bessel functions,

$$\exp(ikx_0 \sin \Omega t) = \sum_{n=-\infty}^{+\infty} J_n(kx_0) \exp(-in\Omega t),$$

Eq. (1.34) can be written as

$$A(t) = A(0) \sum_{n=-\infty}^{+\infty} J_n(kx_0) \exp(-\Gamma_n t/2) \exp(-i\omega_0 t - in\Omega t).$$

Consequently, the normalized distribution of radiation intensity is

$$I(\omega) = I_0 \sum_{n=-\infty}^{+\infty} [J_n(kx_0)]^2 \frac{(\Gamma_n/2)^2}{(\omega - \omega_0 - n\Omega)^2 + (\Gamma_n/2)^2}. \quad (1.35)$$

It is clear that this radiation includes one spectral line unshifted in frequency ( $\omega_0$ ) as well as a series of satellite lines with frequencies  $\omega_0 \pm \Omega$ ,  $\omega_0 \pm 2\Omega$ ,  $\omega_0 \pm 3\Omega$ , etc. Each spectral line has a Lorentzian shape with a width of  $\Gamma_n$ , and its intensity is described by the respective coefficient, i.e., the square of the Bessel function value (Fig. 1.11). Therefore, the recoilless fraction is  $f = [J_0(kx_0)]^2$ .

For a low-energy radiation, we have  $kx_0 \ll 1$ , and

$$\ln f \approx 2 \ln \left( 1 - \frac{k^2 x_0^2}{4} \right) \approx -\frac{k^2 x_0^2}{2}$$

or,

$$f = e^{-k^2 \langle x^2 \rangle} \quad (1.36)$$

where  $\langle x^2 \rangle = x_0^2/2$  is the mean square of the displacement of the nuclear vibration. This result is identical to the quantum mechanical result to be derived next.

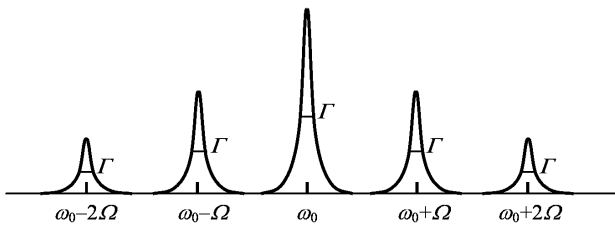


Fig. 1.11 Intensity distribution of  $\gamma$ -ray emission from a classical oscillator.

## 1.5

**The Quantum Theory**

Mössbauer [3] and later Visscher [9] derived the  $f$  fraction based on the theory of neutron resonance scattering from nuclei bound in a solid [10]. Soon after, Lipkin [11] simplified the derivation of the  $f$  fraction. Singwi and Sjölander [12] used a method developed by van Hove [13] to arrive at this result. The reader may find an abundance of relevant references.

In the 1960s, a theoretical method was developed using coherent states [14, 15] (also known as pseudo-classical quantum states). The concept of coherent states has attracted attention from researchers in many areas of physics, and recently found a wide range of applications. The earliest and the most complete studies of the coherent states were those of the harmonic oscillators [16, 17], and these coherent states provide an extremely convenient way of describing certain particular states of vibration. Because harmonic oscillation is an important model for describing the structure and motion of matter on the microscopic scale, the method of coherent states is especially useful in research fields such as studying interactions between radiation and matter. This method not only provides a direct analogy to the classical theory, but also greatly simplifies the calculation. Recently, Bateman et al. [18] calculated the recoilless fraction  $f$  for Mössbauer effect using coherent states. Here, we will use this new approach to the derivation of recoilless fraction  $f$ .

## 1.5.1

**Coherent States of a Harmonic Oscillator**

The Hamiltonian of a one-dimensional harmonic oscillator is

$$\mathcal{H} = \frac{\hat{p}^2}{2m} + \frac{1}{2}m\omega^2\hat{x}^2. \quad (1.37)$$

Instead of using the position and momentum operators  $\hat{x}$  and  $\hat{p}$ , we will introduce an annihilation operator  $\hat{a}$  and a creation operator  $\hat{a}^+$ :

$$\hat{a} = \sqrt{\frac{m\omega}{2\hbar}}\left(\hat{x} + \frac{i}{m\omega}\hat{p}\right), \quad (1.38)$$

$$\hat{a}^+ = \sqrt{\frac{m\omega}{2\hbar}}\left(\hat{x} - \frac{i}{m\omega}\hat{p}\right). \quad (1.39)$$

Solving for  $\hat{x}$  and  $\hat{p}$  from the above definitions, we obtain

$$\hat{x} = \sqrt{\frac{\hbar}{2m\omega}}(\hat{a}^+ + \hat{a}), \quad (1.40)$$

$$\hat{p} = i\sqrt{\frac{m\hbar\omega}{2}}(\hat{a}^+ - \hat{a}). \quad (1.41)$$

Substituting into the Hamiltonian, it becomes quite simple

$$\mathcal{H} = \hbar\omega \left( \hat{a}^+ \hat{a} + \frac{1}{2} \right)$$

and  $\hat{a}^+ \hat{a}$  is known as the number operator  $\hat{N}$ , and its eigenstates  $|n\rangle$  are also eigenstates of the Hamiltonian

$$\mathcal{H}|n\rangle = E_n|n\rangle = \hbar\omega \left( \hat{a}^+ \hat{a} + \frac{1}{2} \right) |n\rangle = \hbar\omega \left( n + \frac{1}{2} \right) |n\rangle \quad n = 0, 1, 2, \dots \quad (1.42)$$

$$\hat{N}|n\rangle = \hat{a}^+ \hat{a}|n\rangle = n|n\rangle. \quad (1.43)$$

This means that each eigenvalue of  $\hat{N}$  is the number of energy quanta  $\hbar\omega$  in the number state  $|n\rangle$ . Any excited state  $|n\rangle$  can be generated by repeatedly applying the creation operator on the ground state  $|0\rangle$ :

$$|n\rangle = \frac{1}{(n!)^{1/2}} (\hat{a}^+)^n |0\rangle \quad (1.44)$$

where all possible  $n$  values are included, and these states  $|n\rangle$  form a complete orthonormal set. We will introduce an important concept, the coherent state, defined as the following linear combination of these states:

$$|\alpha\rangle = e^{-(1/2)|\alpha|^2} \sum_n \frac{\alpha^n}{(n!)^{1/2}} |n\rangle \quad (1.45)$$

where  $\alpha$  may be any complex number, as is proved later. If we substitute (1.44) into (1.45), a coherent state may also be expressed in terms of  $|0\rangle$ :

$$|\alpha\rangle = \hat{D}(\alpha)|0\rangle, \quad (1.46)$$

where  $\hat{D}(\alpha)$  is called the displacement operator

$$\hat{D}(\alpha) = \exp(\alpha \hat{a}^+ - \alpha^* \hat{a}). \quad (1.47)$$

Among all the coherent states ever developed, harmonic oscillator coherent states were the earliest ones and are now the most widely applied. Interestingly, the coherent states represent those states in which the uncertainty relation takes the minimum value (i.e., they describe situations that best resemble classical systems). The squares of standard deviations of position  $x$  and momentum  $p$  are

$$\Delta x^2 = \langle \alpha | x^2 | \alpha \rangle - \langle \alpha | x | \alpha \rangle^2 = \frac{\hbar}{2m\omega}, \quad (1.48)$$

$$\Delta p^2 = \langle \alpha | p^2 | \alpha \rangle - \langle \alpha | p | \alpha \rangle^2 = \frac{\hbar m\omega}{2}. \quad (1.49)$$

The product of the standard deviations is the smallest possible value allowed by the uncertainty principle

$$\Delta x \Delta p = \frac{\hbar}{2}.$$

It is because of this property of satisfying the minimum uncertainty that these quantum states are also known as pseudo-classical coherent states.

For any coherent state, we can show that

$$\hat{a}|\alpha\rangle = \alpha|\alpha\rangle, \quad (1.50)$$

$$\langle\alpha|\hat{a}^+ = \langle\alpha|\alpha^*. \quad (1.51)$$

Since  $\hat{a}$  is not a Hermitian operator,  $\alpha$  is a complex eigenvalue. It is easily verified that the  $|\alpha\rangle$  eigenstates are normalized, but not orthogonal. However, they constitute an overcomplete set, represented by

$$\frac{1}{\pi} \int |\alpha\rangle\langle\alpha| d^2\alpha = \hat{I} \quad (1.52)$$

where  $\hat{I}$  is the unitary operator. This is a very useful operator, because any other operator, particularly the density operator  $\hat{\rho}$ , may be expressed in the coherent state basis as

$$\hat{\rho} = \frac{1}{\pi} \int p(\alpha) |\alpha\rangle\langle\alpha| d^2\alpha. \quad (1.53)$$

This is the  $p$ -representation of the density operator  $\hat{\rho}$ . For oscillators at temperature  $T$  in thermal equilibrium [19]

$$p(\alpha) = \frac{1}{\langle n \rangle} \exp[-|\alpha|^2 / \langle n \rangle] \quad (1.54)$$

where

$$\langle n \rangle = \frac{\exp[-\hbar\omega/k_B T]}{1 - \exp[-\hbar\omega/k_B T]} \quad (1.55)$$

and  $k_B$  is Boltzmann's constant. Therefore, using  $p(\alpha)$  as a weight function, the thermal average of any physical quantity can be evaluated in the coherent state basis.

## 1.5.2

**Gamma Radiation from a Bound Nucleus**

Suppose that an atom is not free but moving in the potential of a harmonic oscillator. Although the motion of this atom may not be identical to that in a crystal, this approximation can lead to the basic characteristics of the Mössbauer effect.

Let the initial state of the atom before irradiating a  $\gamma$ -ray be the ground state  $|0\rangle$  of the harmonic oscillator. As can be seen in (1.42), this state is not an eigenstate of the momentum operator  $\hat{p}$ , and it is impossible to immediately write down its final state through momentum conservation. However, the set of eigenstates of the momentum operator constitute a complete orthonormal set  $|k'\rangle$ , and we may expand  $|0\rangle$  in this set as follows:

$$|0\rangle = \sum |k'\rangle \langle k'|0\rangle. \quad (1.56)$$

When an energy transition occurs within a nucleus at  $t = 0$ , a  $\gamma$ -ray with  $k = E_\gamma/c\hbar$  is emitted in the  $x$ -direction. The momentum of the atom must change from  $\hbar k'$  to  $\hbar(k' - k)$  in order to conserve momentum, and the final state of the atom's motion can be written as

$$|f\rangle = \sum_{k'} |k' - k\rangle \langle k'|0\rangle. \quad (1.57)$$

It is obvious that  $e^{-ik\hat{x}}$  is a displacement operator of  $k$ , thus

$$e^{-ik\hat{x}}|k\rangle = |k' - k\rangle. \quad (1.58)$$

When this is substituted into (1.57), the final state is given by

$$|f\rangle = e^{-ik\hat{x}}|0\rangle. \quad (1.59)$$

Contrary to the case of the free atom, the final state (1.59) is not an eigenstate of the Hamiltonian (1.37) and therefore does not have a well-defined energy. This means that one cannot predict the energy of the  $\gamma$ -ray in advance, but can only provide a probability description. Let us again expand  $|f\rangle$  in the complete set  $|n\rangle$  of eigenstates (1.44):

$$|f\rangle = \sum_n |n\rangle \langle n|f\rangle = \sum_n |n\rangle \langle n|e^{-ik\hat{x}}|0\rangle \quad (1.60)$$

where we have used Eq. (1.59). The probability that the atom is found in the state  $|n\rangle$  with energy  $(n + 1/2)\hbar\omega$  is given by the square of the expansion coefficient in

(1.60). Thus, the probability for the atom to remain in the ground state  $|0\rangle$  after the  $\gamma$ -emission is none other than the recoilless fraction  $f$  of the Mössbauer effect:

$$f = |\langle 0 | e^{-ik\hat{x}} | 0 \rangle|^2. \quad (1.61)$$

To evaluate  $f$ , we express the operator  $e^{-ik\hat{x}}$  in terms of the annihilation operator  $\hat{a}$  and the creation operator  $\hat{a}^+$  by using (1.40)

$$-ik\hat{x} = \alpha\hat{a}^+ - \alpha^*\hat{a} \quad \alpha = -ik\left(\frac{\hbar}{2M\omega}\right)^{1/2} \quad (1.62)$$

where  $M$  is the mass of the nucleus. According to (1.47), the operator  $e^{-ikx}$  happens to be a displacement operator  $\hat{D}$ , and the final state  $|f\rangle$  is a coherent state

$$e^{-ik\hat{x}}|0\rangle = e^{(\alpha\hat{a}^+ - \alpha^*\hat{a})}|0\rangle = |\alpha\rangle = e^{-(1/2)|\alpha|^2} \sum_n \frac{\alpha^n}{(n!)^{1/2}} |n\rangle. \quad (1.63)$$

Applying this to (1.61) and taking account of the orthogonal property of the states  $|n\rangle$ , we obtain

$$f = e^{-|\alpha|^2}.$$

Substituting the value for  $\alpha$  (1.62) into this, we have

$$f = e^{-k^2(\hbar/2M\omega)}. \quad (1.64)$$

As defined in (1.4), the recoil energy is  $E_R = \frac{1}{2}Mv^2 = \frac{p^2}{2M} = \frac{k^2\hbar^2}{2M}$ , and we can express  $f$  in terms of  $E_R$ :

$$f = e^{-E_R/\hbar\omega} \quad (1.65)$$

which is consistent with (1.9).

On the other hand, using a special property of a harmonic oscillator that its average kinetic energy is one half of the total energy (for the ground state, total energy is  $\frac{1}{2}\hbar\omega$ ),

$$\frac{1}{2}M\omega^2\langle x^2 \rangle = \frac{1}{2}\left(\frac{1}{2}\hbar\omega\right), \quad \text{or} \quad \langle x^2 \rangle = \frac{\hbar}{2M\omega}$$

and substituting into (1.64), we obtain

$$f = e^{-k^2\langle x^2 \rangle} \quad (1.66)$$

which is exactly the same as (1.36).

We know that the harmonic oscillator potential well has a parabolic shape. The larger the  $\omega$ -value is, the narrower the potential well, and consequently the Mössbauer nucleus is bound more tightly. Based on the above expressions for the recoilless fraction  $f$ , if  $\omega$  is increased such that  $\hbar\omega \gg E_R$ ,  $\langle x^2 \rangle$  would be very small, and the  $f$ -value could be appreciable.

Finally, it needs to be noted that the recoilless fraction  $f$  can also be expressed in terms of the coherent states  $|\alpha\rangle$ . Since  $\hat{D}^*(\alpha)\hat{D}(\alpha) = 1$ , we can also write formula (1.61) as

$$f = |\langle 0 | e^{-ik\hat{x}} \hat{D}^*(\alpha) \hat{D}(\alpha) | 0 \rangle|^2 = |\langle \alpha | e^{-ik\hat{x}} | \alpha \rangle|^2. \quad (1.67)$$

From the viewpoint of calculating the recoilless fraction  $f$ , both the number state basis and the coherent state basis are identical; the latter, however, has an immense advantage shown in the next section.

### 1.5.3

#### Mössbauer Effect in a Solid

We will now treat the actual situation in the Mössbauer effect where the  $\gamma$ -source nucleus is bound in a solid. Owing to thermal motion, the  $l$ th nucleus is displaced from its equilibrium position  $\mathbf{l}$  by a distance  $\mathbf{u}(l)$ , and therefore its instantaneous position is  $\mathbf{R}_l = \mathbf{l} + \mathbf{u}(l)$ . After it emits a  $\gamma$ -ray, the nucleus makes a transition from its initial state  $|i\rangle$  to the final state  $|f\rangle$ . Because of this, the lattice may have a corresponding transition from its initial phonon state  $|n_i\rangle$  to  $|n_f\rangle$ . The nuclear force causing this transition is the strong force, but its range is extremely short, well within the nucleus itself, and it would not perturb the bonding and motion of the atoms in the solid. On the other hand, the bonding forces between the atoms in the solid are relatively weak, and would have negligible effect on the transition process taking place inside the nucleus. Therefore, these two processes can be considered independent of each other and the overall transition matrix element is the product of the matrix element of the phonon state transition and that of the nuclear transition [18, 19]:

$$\langle n_f | \exp(-i\mathbf{k} \cdot \mathbf{R}_l) | n_i \rangle \langle f | a(\mathbf{k}) | i \rangle.$$

The nuclear transition  $\langle f | a(\mathbf{k}) | i \rangle$  is solely determined by the nuclear properties, regardless of its lattice position. Here, we are only interested in the matrix element describing a phonon state transition from  $|n_i\rangle$  to  $|n_f\rangle$  due to the emission of a  $\gamma$ -photon and a transfer of momentum  $\hbar\mathbf{k}$  from the nucleus to the lattice. The probability of the phonon transition is proportional to

$$p(n_f, n_i) = |\langle n_f | \exp(-i\mathbf{k} \cdot \mathbf{R}_l) | n_i \rangle|^2. \quad (1.68)$$

After summing  $p(n_f, n_i)$  over all possible final states including those in the presence and the absence of recoil, we find the normalization condition:

$$\begin{aligned}
& \sum_f |\langle n_f | \exp(-i\mathbf{k} \cdot \mathbf{R}_l) | n_i \rangle|^2 \\
&= \sum_f \langle n_i | \exp(i\mathbf{k} \cdot \mathbf{R}_l) | n_f \rangle \langle n_f | \exp(-i\mathbf{k} \cdot \mathbf{R}_l) | n_i \rangle = 1.
\end{aligned} \tag{1.69}$$

The relative probability of  $\gamma$ -emission without recoil is the recoilless fraction  $f$  written as

$$f = \sum_f |\langle n_f | \exp(-i\mathbf{k} \cdot \mathbf{R}_l) | n_i \rangle|^2 \delta(E_f - E_i). \tag{1.70}$$

At temperature  $T$ , the initial phonon states may follow a particular distribution  $p_{n_i}(T)$ , and Eq. (1.70) is then multiplied by  $p_{n_i}(T)$  and summed over all initial states  $n_i$ . For the sake of simplicity, we assume that the equilibrium position of the radioactive nucleus to be at the origin, thus  $\mathbf{R}_l = \mathbf{u}(l)$ , and

$$\begin{aligned}
f &= \sum_i \sum_f p_{n_i}(T) |\langle n_f | \exp(-i\mathbf{k} \cdot \mathbf{u}(l)) | n_i \rangle|^2 \delta(E_f - E_i) \\
&= |\langle\langle n_i | \exp(-i\mathbf{k} \cdot \mathbf{u}(l)) | n_i \rangle\rangle_T|^2
\end{aligned} \tag{1.71}$$

where  $\langle\langle \dots \rangle\rangle_T$  represents the thermal average.

In order to evaluate  $f$  in the coherent state basis, we start by expressing the component of  $\mathbf{u}(l)$  in the  $\mathbf{k}$ -direction through the normal coordinates  $q_s$  ( $s = 1, 2, 3, \dots, 3N$ ) as

$$u_k(l) = \frac{1}{\sqrt{M}} \sum_{s=1}^{3N} B_k(l, s) q_s, \tag{1.72}$$

with the normalization condition

$$\sum_{s=1}^{3N} |B_k(l, s)|^2 = 1. \tag{1.73}$$

Each  $q_s$  may be represented by the operators  $\hat{a}_s^+$  and  $\hat{a}_s$ :

$$q_s = \sqrt{\frac{\hbar}{2\omega_s}} (\hat{a}_s^+ + \hat{a}_s), \tag{1.74}$$

where  $\omega_s$  is the  $s$ th modal angular frequency. For a crystal of  $3N$  independent normal mode oscillators, we must use the product of  $3N$  individual coherent states  $|\{\alpha_s\}\rangle \equiv \prod_s |\alpha_s\rangle$  instead of the number states in (1.71), and

$$f = |\langle\langle \{\alpha_s\} | e^{-i\mathbf{k} \cdot \mathbf{u}(l)} | \{\alpha_s\} \rangle\rangle_T|^2. \tag{1.75}$$

The matrix elements may be written as follows:

$$\begin{aligned} & \langle \{\alpha_s\} | e^{-i\mathbf{k} \cdot \mathbf{u}(l)} | \{\alpha_s\} \rangle \\ &= \prod_s \langle \alpha_s | \exp \left[ -ik \left( \frac{\hbar}{2M\omega_s} \right)^{1/2} B_k(l, s) (\hat{\mathbf{a}}_s^+ + \hat{\mathbf{a}}_s) \right] | \alpha_s \rangle. \end{aligned} \quad (1.76)$$

Since the operators  $\hat{\mathbf{a}}_s^+$  and  $\hat{\mathbf{a}}_s$  do not commute, but  $[\hat{\mathbf{a}}_s^+, \hat{\mathbf{a}}_s] = -1$ , we apply Glauber's formula

$$e^{\hat{\mathbf{a}}_s^+ + \hat{\mathbf{a}}_s} = e^{\hat{\mathbf{a}}_s^+} e^{\hat{\mathbf{a}}_s} e^{-(1/2)[\hat{\mathbf{a}}_s^+, \hat{\mathbf{a}}_s]} \quad (1.77)$$

to simplify (1.76). Letting  $k(\hbar/2M\omega_s)^{1/2} B_k(l, s) = \rho_s$ , we have

$$e^{-i\rho_s(\hat{\mathbf{a}}_s^+ + \hat{\mathbf{a}}_s)} = e^{-i\rho_s \hat{\mathbf{a}}_s^+} e^{-i\rho_s \hat{\mathbf{a}}_s} e^{-(1/2)\rho_s^2}. \quad (1.78)$$

Substituting this into (1.76) and using properties of coherent states ((1.50) and (1.51)), each factor in the product of (1.76) becomes

$$\langle \alpha_s | \exp[-i\rho_s(\hat{\mathbf{a}}_s^+ + \hat{\mathbf{a}}_s)] | \alpha_s \rangle = e^{-(1/2)\rho_s^2} e^{-i\rho_s(\alpha_s^* + \alpha_s)}$$

and the matrix element is

$$\langle \{\alpha_s\} | e^{-i\mathbf{k} \cdot \mathbf{u}(l)} | \{\alpha_s\} \rangle = \exp \left[ -\frac{1}{2} \sum_s \rho_s^2 \right] \exp \left[ -2i \sum_s \rho_s \operatorname{Re}(\alpha_s) \right]. \quad (1.79)$$

The next step is to take a thermal average  $\langle \cdots \rangle_T$  over the probability of a particular distribution  $p(\alpha_s)$  as described in (1.54), and we have

$$\begin{aligned} \langle \cdots \rangle_T &= \int \langle \cdots \rangle p(\alpha_s) d^2 \alpha_s \\ &= \exp \left[ -\frac{1}{2} \sum_s \rho_s^2 \right] \prod_s \int \frac{d^2 \alpha_s}{\pi \langle n_s \rangle} \exp \left[ -\frac{|\alpha_s|^2}{\langle n_s \rangle} \right] \exp[-2i\rho_s \operatorname{Re}(\alpha_s)]. \end{aligned}$$

Letting  $\alpha_s = \zeta + i\eta$ ,

$$\begin{aligned} \langle \cdots \rangle_T &= \exp \left[ -\frac{1}{2} \sum_s \rho_s^2 \right] \exp \left[ -\sum_s \rho_s \langle n_s \rangle \right] \\ &\times \prod_s \int_{-\infty}^{+\infty} \frac{1}{(\pi \langle n_s \rangle)^{1/2}} \exp \left[ -\frac{1}{\langle n_s \rangle} (\zeta + i\rho_s \langle n_s \rangle)^2 \right] d\zeta \\ &\times \prod_s \int_{-\infty}^{+\infty} \frac{1}{(\pi \langle n_s \rangle)^{1/2}} \exp \left[ -\frac{1}{\langle n_s \rangle} \eta^2 \right] d\eta \end{aligned}$$

$$\begin{aligned}
&= \exp \left[ - \sum_s \rho_s^2 \left( \langle n_s \rangle + \frac{1}{2} \right) \right] \\
&= \exp \left[ - \frac{E_R}{2} \sum_s \frac{|B_k(l, s)|^2}{\hbar \omega_s} \coth \left( \frac{\hbar \omega_s}{2k_B T} \right) \right].
\end{aligned} \tag{1.80}$$

The two integrals in the above calculations are Gaussian integrals:  $\langle n_s \rangle$  is the average phonon number at  $T$  defined in (1.55) and  $E_R = \hbar^2 k^2 / (2M)$  corresponds to the recoil energy of the free nucleus. Using (1.80), the recoilless fraction in (1.75) is reduced to

$$f = \exp \left[ -E_R \sum_s \frac{|B_k(l, s)|^2}{\hbar \omega_s} \coth \left( \frac{\hbar \omega_s}{2k_B T} \right) \right]. \tag{1.81}$$

This still contains a summation over different normal modes, but it may be replaced by a frequency integral over density of states  $g(\omega)$ . For a cubic crystal, it is only necessary to consider one displacement component, and the corresponding coefficient  $|B_k(l, s)|^2$  is equal to  $1/(3N)$  (see Eq. (8.63)). Therefore, we have the final result for  $f$ :

$$f = \exp \left[ -E_R \int \frac{g(\omega)}{\hbar \omega} \coth \left( \frac{\hbar \omega}{2k_B T} \right) d\omega \right] \tag{1.82}$$

where  $g(\omega)$  is normalized to unity.

For an Einstein lattice and for  $T \rightarrow 0$ , Eq. (1.81) becomes (1.65). Further evaluation of  $f$  in a general case requires the knowledge of  $g(\omega)$ . A more realistic model is the Debye model whose density of states is

$$g(\omega) = \frac{3\omega^2}{\omega_D^3} \quad (\omega < \omega_D), \tag{1.83}$$

and in this case

$$f = \exp \left\{ - \frac{3E_R}{2k_B \theta_D} \left[ 1 + 4 \left( \frac{T}{\theta_D} \right)^2 \int_0^{\theta_D/T} \frac{x dx}{(e^x - 1)} \right] \right\} \tag{1.84}$$

where  $x = \hbar \omega / k_B T$  and  $\theta_D = \hbar \omega_D / k_B$  is the Debye temperature. This is an approximate formula of the recoilless fraction  $f$  that is often used in practice.

Here again we have demonstrated the equivalency of phonon number states  $|n\rangle$  and the coherent states  $|\alpha\rangle$ , when they are used in calculating  $f$ . In principle, other basis functions, if possible, may also be used, provided they satisfy the requirement that the energy state of the crystal is not changed after the  $\gamma$ -ray emission. However, one can see from Sections 1.5.2 and 1.5.3 that the derivation using

coherent states is not only simpler (Gaussian integrals are all one needs to use), but also more rigorous (because no approximation was made for the derivation of (1.81)). In addition, coherent states are those quantum states that are most similar to classical situations, and their applications in the derivation of  $f$  indicates that there is a classical correspondence in the Mössbauer effect. It is then not surprising that in Section 1.4 the classical radiation theory was able to give a recoilless fraction  $f$  that is identical to Eq. (1.66).

#### 1.5.4

##### Average Energy Transferred

In the source, a large number of excited Mössbauer nuclei (e.g.,  $^{57}\text{Fe}$ ) are imbedded in a crystal lattice. During the  $\gamma$ -emission, the average energy transferred to the lattice is exactly equal to the recoil energy for a free nucleus  $E_R$  [20, 21]. This was first proved by Lipkin [11], and it is known as Lipkin's sum rule, which we discuss again in Chapter 7.

Suppose that the interactions between the atoms in the lattice are dependent only on their positions, but not on their velocities. The only term in the lattice Hamiltonian that does not commute with  $\exp(i\mathbf{k} \cdot \mathbf{u}(l))$  is the kinetic energy operator  $\hat{\mathbf{p}}^2/(2M)$  of the emitting nucleus. Accordingly,

$$\begin{aligned} [\mathcal{H}, \exp(i\mathbf{k} \cdot \mathbf{u}(l))] &= \left[ \frac{\hat{\mathbf{p}}^2}{2M}, \exp(i\mathbf{k} \cdot \mathbf{u}(l)) \right] \\ &= \exp(i\mathbf{k} \cdot \mathbf{u}(l)) \left( \frac{\hbar^2 k^2}{2M} + \frac{\hbar \mathbf{k} \cdot \hat{\mathbf{p}}}{M} \right). \end{aligned} \quad (1.85)$$

Utilizing

$$e^{\pm i\mathbf{k} \cdot \mathbf{u}(l)} \hat{\mathbf{p}} e^{\mp i\mathbf{k} \cdot \mathbf{u}(l)} = \hat{\mathbf{p}} \pm \hbar \mathbf{k},$$

we can calculate the double commutator

$$[[\mathcal{H}, \exp(i\mathbf{k} \cdot \mathbf{u}(l))], \exp(-i\mathbf{k} \cdot \mathbf{u}(l))] = -\frac{\hbar^2 k^2}{M} = -2E_R. \quad (1.86)$$

On the other hand, this commutator can also be written as

$$\begin{aligned} &[[\mathcal{H}, \exp(i\mathbf{k} \cdot \mathbf{u}(l))], \exp(-i\mathbf{k} \cdot \mathbf{u}(l))] \\ &= 2\mathcal{H} - \exp(i\mathbf{k} \cdot \mathbf{u}(l)) \mathcal{H} \exp(-i\mathbf{k} \cdot \mathbf{u}(l)) \\ &\quad - \exp(-i\mathbf{k} \cdot \mathbf{u}(l)) \mathcal{H} \exp(i\mathbf{k} \cdot \mathbf{u}(l)). \end{aligned} \quad (1.87)$$

If we calculate the expectation value of this commutator when the system is at its initial state  $|n_i\rangle$  with energy  $E_i$ , we get

$$\begin{aligned}
& \langle n_i | [[\mathcal{H}, \exp(i\mathbf{k} \cdot \mathbf{u}(l))], \exp(-i\mathbf{k} \cdot \mathbf{u}(l))] | n_i \rangle \\
&= 2E_i - \sum_f \langle n_i | \exp(i\mathbf{k} \cdot \mathbf{u}(l)) | n_f \rangle \langle n_f | \mathcal{H} \exp(-i\mathbf{k} \cdot \mathbf{u}(l)) | n_i \rangle \\
&\quad - \sum_f \langle n_i | \exp(-i\mathbf{k} \cdot \mathbf{u}(l)) | n_f \rangle \langle n_f | \mathcal{H} \exp(i\mathbf{k} \cdot \mathbf{u}(l)) | n_i \rangle \\
&= 2E_i - 2 \sum_f E_f |\langle n_f | \exp(-i\mathbf{k} \cdot \mathbf{u}(l)) | n_i \rangle|^2
\end{aligned} \tag{1.88}$$

where a complete set of final states  $|n_f\rangle$  was inserted. Taking into account Eqs. (1.68), (1.69), (1.86), and (1.88), we arrive at Lipkin's sum rule

$$\sum_f (E_f - E_i) p(n_f, n_i) = E_R. \tag{1.89}$$

When  $i = f$ ,  $E_R = 0$ ,  $p(n_i, n_i)$  is none other than the recoilless fraction  $f$ , i.e., the portion of the  $\gamma$ -ray emission process that has no energy exchange with the lattice. The rest of the emission process will cause recoil, whose recoil energy will have to be sufficiently large so that the average energy transferred to the lattice is  $E_R$ .

In order to obtain a relatively large  $f$  value, the Mössbauer nucleus should be tightly bound in a localized potential well to form a localized state, and the Debye temperature  $\theta_D$  should be as high as possible. One of the best examples is the  $^{57}\text{Fe}$  impurities in diamond [22]. Diamond has the highest known Debye temperature  $\theta_D = 2230$  K, and  $f(295 \text{ K}) = 0.94 \pm 0.06$  [23], which is probably the highest recoilless fraction at room temperature ever detected thus far.

## References

- 1 W. Kuhn. Scattering of thorium C''  $\gamma$ -radiation by radium G and ordinary lead. *Phil. Mag.* 8, 625–636 (1929).
- 2 P.B. Moon and A. Storruste. Resonant nuclear scattering of  $^{198}\text{Hg}$  gamma-rays. *Proc. Phys. Soc. (London)* 66, 585–589 (1953).
- 3 R.L. Mössbauer. Kernresonanzfluoreszenz von Gammastrahlung in  $\text{Ir}^{191}$ . *Z. Phys.* 151, 124–143 (1958); R.L. Mössbauer. Kernresonanzabsorption von Gammastrahlung in  $\text{Ir}^{191}$ . *Naturwiss.* 45, 538–539 (1958).
- 4 J.M. Williams and J.S. Brooks. The thickness dependence of Mössbauer absorption line areas in unpolarized and polarized absorbers. *Nucl. Instrum. Methods* 128, 363–372 (1975).
- 5 Chen Yi-long, Lu Ning, Peng Li-li, and Zhao Lei. An exact expression for fractional absorption in Mössbauer spectroscopy. *Wuhan University J. Natur. Sci.* 6, 784–786 (2001).
- 6 S.L. Ruby and J.M. Hicks. Line shape in Mössbauer spectroscopy. *Rev. Sci. Instrum.* 33, 27–30 (1962).
- 7 R.M. Housley, N.E. Erickson, and J.G. Dash. Measurement of recoil-free fractions in studies of the Mössbauer effect. *Nucl. Instrum. Methods* 27, 29–37 (1964).

- 8 F.L. Shapiro. The Mössbauer effect. *Soviet Physics Uspekhi* 4, 881–887 (1961) [Russian original: *Uspekhi Fiz. Nauk* 72, 685–696 (1960)].
- 9 W.M. Visscher. Study of lattice vibrations by resonance absorption of nuclear gamma rays. *Ann. Phys.* 9, 194–210 (1960).
- 10 W.E. Lamb. Capture of neutrons by atoms in a crystal. *Phys. Rev.* 55, 190–197 (1939).
- 11 H.J. Lipkin. Some simple features of the Mössbauer effect. *Ann. Phys.* 9, 332–339 (1960).
- 12 K.S. Singwi and A. Sjölander. Resonance absorption of nuclear gamma rays and the dynamics of atomic motions. *Phys. Rev.* 120, 1093–1102 (1960).
- 13 L. Van Hove. Correlations in space and time and Born approximation scattering in systems of interacting particles. *Phys. Rev.* 95, 249–262 (1954).
- 14 R.J. Glauber. Coherent and incoherent states of the radiation field. *Phys. Rev.* 131, 2766–2788 (1963).
- 15 C. Cohen-Tannoudji, B. Diu, and F. Laloë. *Quantum Mechanics*, vol. 1, p. 295 (John Wiley, New York, 1977).
- 16 S. Howard and S.K. Roy. Coherent states of a harmonic oscillator. *Am. J. Phys.* 55, 1109–1117 (1987).
- 17 R. Loudon. *The Quantum Theory of Light*, pp. 148–153 (Oxford University Press, Oxford, 1973).
- 18 D.S. Bateman, S.K. Bose, B. Dutta-Roy, and M. Bhattacharyya. The harmonic lattice, recoilless transitions, and the coherent state. *Am. J. Phys.* 60, 829–832 (1992).
- 19 R.J. Glauber. *Quantum Optics*, pp. 15–56 (Academic Press, New York, 1969).
- 20 J. Callaway. *Quantum Theory of the Solid State* (Academic Press, New York, 1974).
- 21 C. Kittel. *Quantum Theory of Solids*, p. 389 (John Wiley, New York, 1963).
- 22 J.A. Sawicki and B.D. Sawicka. Properties of  $^{57}\text{Fe}$  hot-implanted into diamond crystals studied by Mössbauer emission spectroscopy between 4 and 300 K. *Nucl. Instrum. Methods B* 46, 38–45 (1990).
- 23 T.W. Sinor, J.D. Standifird, F. Davanloo, K.N. Taylor, C. Hong, J.J. Carroll, and C.B. Collins. Mössbauer effect measurement of the recoil-free fraction for  $^{57}\text{Fe}$  implanted in a nanophase diamond film. *Appl. Phys. Lett.* 64, 1221–1223 (1994).

